Cassini Imaging Science: Initial Results on Saturn's Atmosphere

C. C. Porco,[1]* E. Baker,[1] J. Barbara,[2] K. Beurle,[3] A. Brahic,[4] J. A. Burns,[5] S. Charnoz,[4] N. Cooper,[3] D. D. Dawson,[6] A. D. Del Genio,[2] T. Denk,[7] L. Dones,[8] U. Dyudina,[9] M. W. Evans,[3] B. Giese,[10] K. Grazier,[11] P. Helfenstein,[5] A. P. Ingersoll,[9] R. A. Jacobson,[11] T. V. Johnson,[11] A. McEwen,[6] C. D. Murray,[3] G. Neukum,[7] W. M. Owen,[11] J. Perry,[6] T. Roatsch,[10] J. Spitale,[1] S. Squyres,[5] P. Thomas,[5] M. Tiscareno,[5] E. Turtle,[6] A. R. Vasavada,[11] J. Veverka,[5] R. Wagner,[10] R. West[11]

The Cassini Imaging Science Subsystem (ISS) began observing Saturn in early February 2004. From analysis of cloud motions through early October 2004, we report vertical wind shear in Saturn's equatorial jet and a maximum wind speed of ~375 meters per second, a value that differs from both Hubble Space Telescope and Voyager values. We also report a particularly active narrow southern mid-latitude region in which dark ovals are observed both to merge with each other and to arise from the eruptions of large, bright storms. Bright storm eruptions are correlated with Saturn's electrostatic discharges, which are thought to originate from lightning.

During the Voyager flybys of the giant planets in the 1980s, Saturn was probably the windiest planet in the solar system (1). Its equatorial jet flowed eastward at 470 m s^{-1} (2), which is more than 10 times the speed of Earth's tropospheric jet streams. The jets are powered partly by solar energy and partly by internal heat; their sum is ~1.8 times the globally averaged absorbed solar energy. The solar irradiance is 1% that at Earth. Saturn's atmosphere is mostly H_2 and He, with small amounts of CH_4, NH_3, PH_3, and presumably H_2S and H_2O, although the last two are frozen out below the cloud tops and are undetectable by the usual remote sensing methods. On the basis of solar elemental abundances, the inferred abundance of oxygen (and hence of water) in the deep atmosphere is sufficient to support moist convection, precipitation, and lightning.
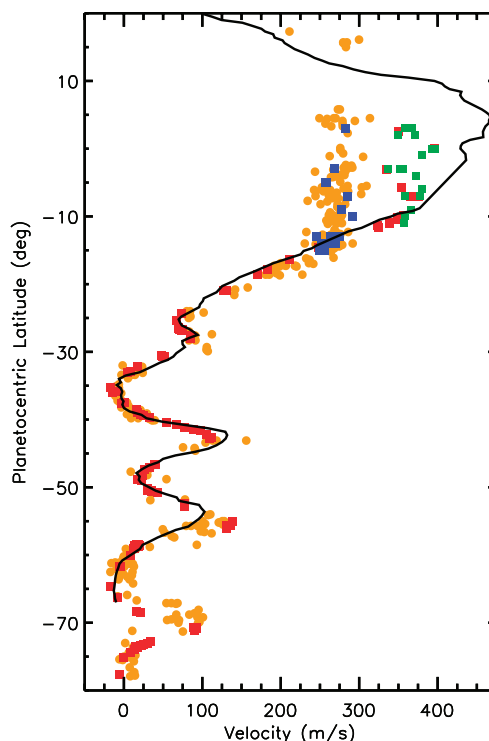
On Saturn, the wind is defined as the velocity relative to the System III reference frame

(3), which rotates at a fixed period of 10 hours 39 min 24 s. This was the period of Saturn's kilometric radio (SKR) emissions at the time of the Voyager flybys in 1980–1981. Since then the SKR period has varied by 1% (4) and is currently 10 hours 45 min 45 s (5). In addition, Hubble Space Telescope (HST) observations from 1996 to 2004 indicate that the equatorial jet slowed to ~275 m s^{-1} relative to System III (2, 6, 7). Any real slowing of the winds might be connected to the extreme seasonal cycles of insolation (sunlight incident on a horizontal surface) as the shadow of the rings moves from one hemisphere to the other (8, 9), or to the

extreme outbursts of cloud activity, the last of which disrupted the appearance of the equatorial zone (EZ) between 1990 and 1997 (10–12). It is also possible that the winds are constant in time but the altitude of the visible clouds has increased, revealing slower speeds at higher levels (10, 12, 13). We focus on the last hypothesis.

The ISS cameras imaged Saturn's atmosphere regularly between 6 February and 12 May 2004, and again on 29–30 May 2004 during Cassini's final approach to Saturn (14) and in September during the first orbit of Saturn. The long time baseline and the wide spectral range of the ISS cameras, from the near-infrared (near-IR) to the ultraviolet, are ideal for discriminating clouds and hazes at various altitudes and for monitoring winds, vortices, and evolving cloud structures (15, 16). Coverage in the southern hemisphere was complete, but the northern hemisphere was obscured by the shadow of Saturn's rings (17).

We measured wind speeds by tracking the displacements of spots and cloud/haze features

[1]Cassini Imaging Central Laboratory for Operations, Space Science Institute, 4750 Walnut Street, Suite 205, Boulder, CO 80301, USA. [2]Goddard Institute for Space Studies, NASA, 2880 Broadway, New York, NY 10025, USA. [3]Astronomy Unit, Queen Mary, University of London, London E1 4NS, UK. [4]Centre d'Etudes de Saclay, Université Paris 7, L'Orme des Merisiers, 91191 Gif-sur-Yvette Cedex, France. [5]Department of Astronomy, Cornell University, Space Sciences Building, Ithaca, NY 14853, USA. [6]Department of Planetary Sciences, University of Arizona, 1629 East University Boulevard, Tucson, AZ 85721, USA. [7]Institut für Geologische Wissenschaften, Freie Universität, 12249 Berlin, Germany. [8]Department of Space Sciences, Southwest Research Institute, 1050 Walnut Street, Suite 400, Boulder, CO 80302, USA. [9]Division of Geological and Planetary Sciences, California Institute of Technology, 150-21, Pasadena, CA 91125, USA. [10]Institute of Planetary Research, German Aerospace Center, Rutherfordstrasse 2, 12489 Berlin, Germany. [11]Jet Propulsion Laboratory, California Institute of Technology, 4800 Oak Grove Drive, Pasadena, CA 91109, USA.

*To whom correspondence should be addressed. E-mail: carolyn@ciclops.org

Fig. 1. Zonal winds (positive eastward) in Saturn's atmosphere. Winds in the equatorial region vary over time and with image wavelength. Measurements made by Voyagers 1 and 2 in 1980–1981 through the green filter (2) are the fastest (solid line). Winds derived from 1996–2004 HST images (7) are slower and independent of wavelength (orange circles). Cassini measurements at 750 nm, made by two authors (red and green squares), fall between those of Voyager and HST. Cassini measurements at 727 nm (blue squares) are close to those of HST. Winds south of 15°S show few changes from 1980–1981 (Voyager, solid line) (2) to 1996–2004 (HST, orange circles) (7) to 2004 (Cassini at 750 nm, red squares). Voyager observations extend only to 65°S and do not reveal the jet near 70°S.

in Cassini images separated by either 10.5 or 21 hours (*18*). The speeds of the zonal winds poleward of 15°S latitude are similar to those measured during the Voyager and HST eras (Fig. 1). The zonal (eastward) velocity has local maxima at 27°, 43°, 55°, and 70°S. There are zonal velocity minima at 35°, 48°, and 65°S. Images taken in the deep-sounding continuum CB2 (750 nm) filter give equatorial jet speeds of 325 to 400 m s^{-1}, which falls between the Voyager and HST estimates. Images taken in the gaseous methane absorption band MT2 (727 nm) filter, which senses higher altitudes, give equatorial jet speeds of 250 to 300 m s^{-1}, in

agreement with the HST result (Fig. 1). This relation between the measured wind speed and the altitude to which the filter is sensitive was first noticed in HST images after the 1990 equatorial disturbance and was interpreted as evidence of vertical shear in the zonal winds (*10*). For the HST data from 1996 to 2004, the large high-contrast features in the EZ emerged in the strong methane band (890 nm). The authors of the 1996–2004 study estimate that the EZ features' average level was $P \sim 45$ mbar in 2003 and was ~ 300 mbar during the Voyager era (*7*).

The equatorial velocities from the Voyager, HST, and Cassini data imply vertical wind shear.

The MT2 filter is centered on a methane absorption band, so clouds are visible only if they are at high altitude—above most of the methane gas. The CB2 filter is outside the methane bands, so clouds are visible at all levels. Optically thin clouds at high altitude will be more visible in the MT2 filter, where the methane gas provides a dark background, and they will be less visible in the CB2 filter, where bright deep clouds provide the background. Figure 2 shows an example of different features appearing in different filters at the same time and place on the planet.

Wind speed observations from Voyager were determined by tracking clouds seen in

Fig. 2. Near-simultaneous views in different filters of the same place on the planet. The upper left and right images use the CB2 filter (750 nm), where the gases absorb weakly; the lower left and right images use the MT2 filter (727 nm), where methane absorbs more strongly. The left images were taken within 1 min of each other and cover the same latitude-longitude range. They were taken 10 hours 30 min before the right images, which were also taken within 1 min of each other and also cover the same latitude-longitude range. The velocities measured by tracking the features (arrows) in the CB2 images (top) are

$\sim$100 m s^{-1} faster than those in the MT2 images (bottom).
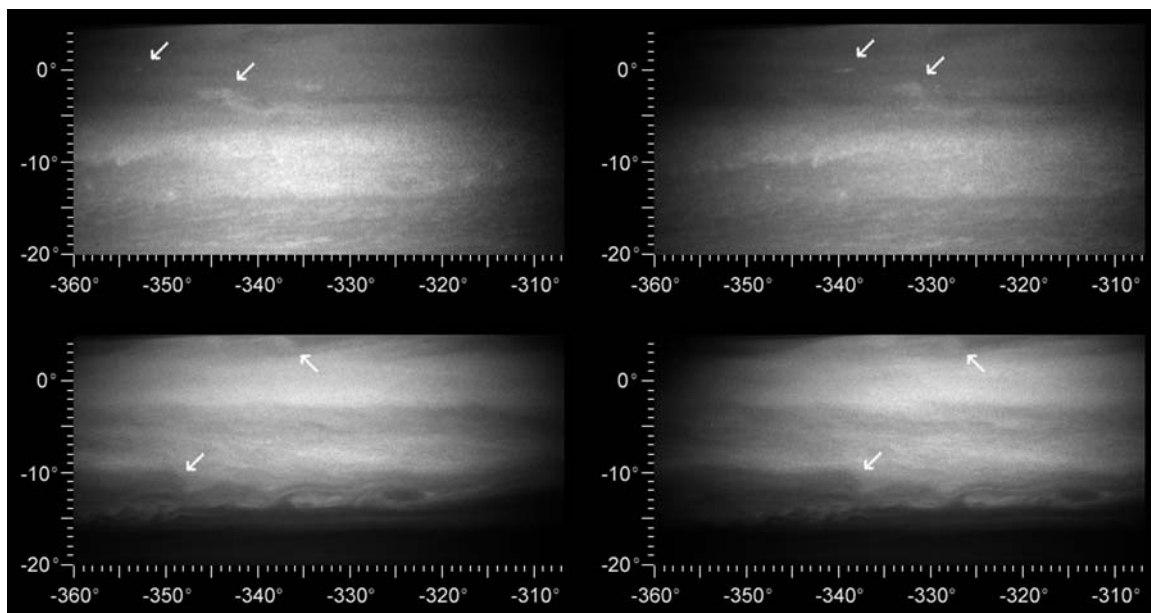
Fig. 3. Two storms, with diameters close to 1000 km, were captured in the act of merging during Cassini's approach to Saturn. Both storms, which appear as spots in the southern hemisphere, were seen moving westward, relative to System III, for about a month before they merged on 19–20 March 2004. The series of eight images shown here was taken between 22 February and 22 March

2004; the image scale ranges from 381 km (237 miles) to 300 km (186 miles) per pixel. All images have been processed to enhance visibility. The top four frames, spanning 26 days, are portions of narrow-angle camera images that were taken through a filter accepting light in the near-IR region of the spectrum centered at 619 nm, and show two spots approaching each other. Both storms are within half a degree of 36°S latitude and sit in an anticyclonic shear zone, which means that the flow to the north is westward relative to the flow to the south. Consequently, the northern storm moves westward at 11 m s^{-1}, a slightly greater rate
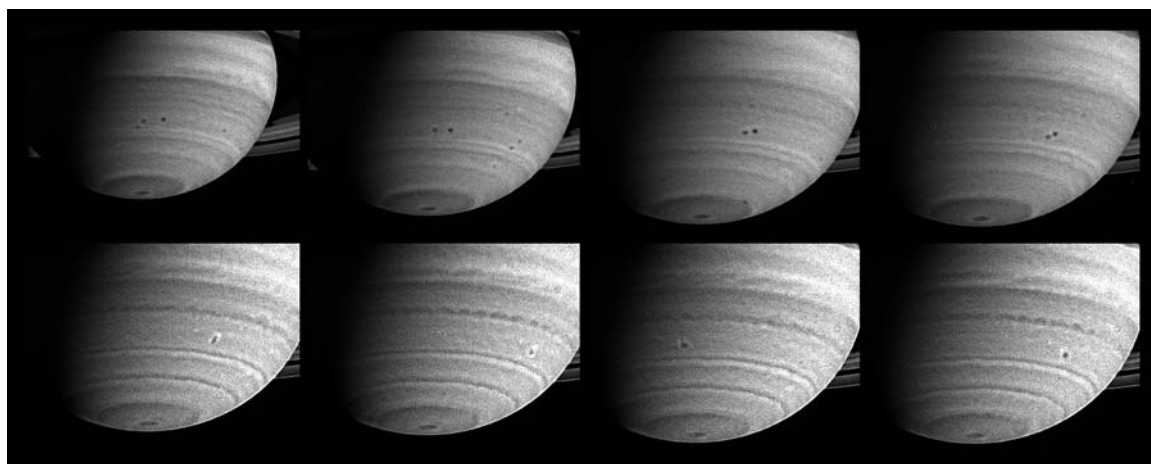
than the southern one (6 m s^{-1}). The storms drift with these currents and engage in a counterclockwise dance before merging with each other. The bottom four frames are from images taken on 19, 20, 21, and 22 March, respectively, in a region of the spectrum visible to the human eye and illustrate the storms' evolution. Just after the merger, on 19 March, the new feature is elongated in the north-south direction, with bright clouds on either end. Two days later, on 22 March, it has settled into a more circular shape and the bright clouds have spread around the circumference to form a halo.

the Voyager green filter, which senses approximately the same altitude as the CB2 filter. The 100 m s^{-1} difference in equatorial speeds between the CB2 and MT2 filters is consistent with winds decreasing with height coupled with thin high clouds. Retrievals of haze altitudes support the idea that the 1990–1997 equatorial storms put haze particles at higher altitudes than during the Voyager years. The pressure at the top of the main haze layer appears to have decreased from ~200 mbar in 1979 (19) to about 70 mbar in 2002 (20).

Retrievals of temperature support the idea that the zonal wind speed decreases with height. The Cassini Composite Infrared Spectrometer (CIRS) team (13) observed an increase in temperature toward the south pole, which implies that the zonal winds decay with height according to the thermal wind equation. This equation is singular at the equator, so the wind shear profile stops at 5°S. If the Voyager wind profile holds at the 500-mbar level, at 5°S the winds will reach 275 m s^{-1} at the 3-mbar level, and at 10°S they will reach 275 m s^{-1} at the 30-mbar level. These altitudes are higher than the 45- and 70-mbar estimates given earlier for the stratospheric haze, but they are within the combined uncertainty of estimating the altitude of features from methane band filters and applying the thermal wind equation within 5° of the equator.

The westward jet at 35°S planetocentric latitude (Fig. 1) was the most active region of the planet during Cassini's long approach to Saturn in the first half of 2004 (7). Voyager 2 observed similar activity in 1980–1981 near the westward jet at 34°N (21). "Activity" is here defined to mean having a dozen or more compact oval spots with diameters larger than 500 km and lifetimes longer than a week. At 35°S, most of the spots sat in the shear zone just to the south of the jet. Spots in the jet moved westward at speeds up to 25 m s^{-1}. Spots a few degrees to the south moved eastward at comparable speeds. The spots themselves rotated counterclockwise (anticyclonic in the southern hemisphere), like ball bearings between conveyor belts, with the same sense of rotation as the ambient shear flow. It was not possible to determine the sense of rotation for all the spots, especially the smallest ones, but the impression from movies of time-lapse images (movies S1 and S2) is that they were all anticyclonic. The jet at the zonal velocity minimum at 48°S was also active and exhibited the same phenomena, with anticyclonic vortices rolling in the anticyclonic shear zone to the south of the jet.

The interaction of westward-moving and eastward-moving spots in adjacent latitude bands sometimes produced a merger (Fig. 3) or a near-merger, with bright material suddenly forming between the two spots or around them. Further analysis of the images taken in different spectral filters will show whether the bright material consists of particles of a different composition, size, or altitude. The compact spots were mostly dark, but they often had bright halos. The new spot that resulted from a merger sometimes continued on for weeks and sometimes split apart after a few days. Because mergers represent a net decrease in the number of spots, there must be another process that causes the spots to form. Figures 4 and 5 show one possibility. In Fig. 4, the first six frames show a large eruption of bright white clouds in the 35°S latitude band. The eruption, which suggests moist convection, later produces three dark stable spots where there were none before. In Fig. 5, days 272 and 274 record the curling of a dark filament on its way to becoming a dark spot. These observations may indicate that moist convection, through the injection of vorticity at cloud level, supplies energy to maintain the jets on jovian planets (22).

Linear bands encircle the planet, each with its own mottled texture. The edges of the bands are wave-like and often break into turbulent eddies. On the largest scale, rotational symmetry is the dominant feature (Fig. 3). A curious manifestation of this symmetry occurs at the south pole, where a small (2000 km diameter) feature sits undisturbed. The precise alignment suggests that the perturbing forces are small.

One storm at 35°S produced eruptions of white material in mid-July and again in mid-September (Fig. 5). During these eruptions, the Radio and Plasma Wave Science (RPWS) instrument (3, 5, 23) was detecting Saturn electrostatic discharges (SEDs), which are short bursts—tens of milliseconds in duration—with large bandwidth, spanning 2 to 40 MHz in frequency. The SEDs are different from SKR radiation, although both are radio waves. The SED bursts are grouped into episodes that recur with a distinct periodicity (~10 hours 40 min), which is approximately equal to the System III rotation period. Voyagers 1 and 2 also detected SEDs, which were also grouped into episodes, but the recurrence period was ~10 hours 10 min (3). The bursts may have originated in the rings, and they may have originated in the atmosphere (24). The Cassini data favor an atmospheric origin (i.e., lightning).

The Voyager and Cassini periods for the SEDs are close to the minimum and maximum recurrence intervals, respectively, for atmospheric features crossing the center of the planetary disk—the central meridian (CM)—as viewed by a stationary observer. The shorter period is characteristic of the high-speed equatorial jet. The longer period is characteristic of the spots just south of the westward jet at 35°S, where the storm erupted in July and September 2004. We matched the phase of the SED bursts with the times that the storm crossed the CM over a period spanning 58 rotations of the planet, which is more than 25 days. A constant relative phase

Fig. 4. Spots merging and spots arising. Each panel shows a region in the vicinity of the westward jet at 35°S taken from one of the maps that constitute the cylindrical movie (movie S2) of Saturn's southern hemisphere. The time shown is that of the first of the six images that make up each cylindrical map (14); the actual time the region was imaged is within one rotation period after the time shown. In the first six frames, two dark spots merge (on approximately day 86, 26 March 2004) after spiraling toward each other in a counterclockwise direction. In the last seven frames, three dark spots arise from the remnants of the bright white storm seen in the earlier frames and spin around each other. Two of the newly developed spots merge between day 107 and day 110.
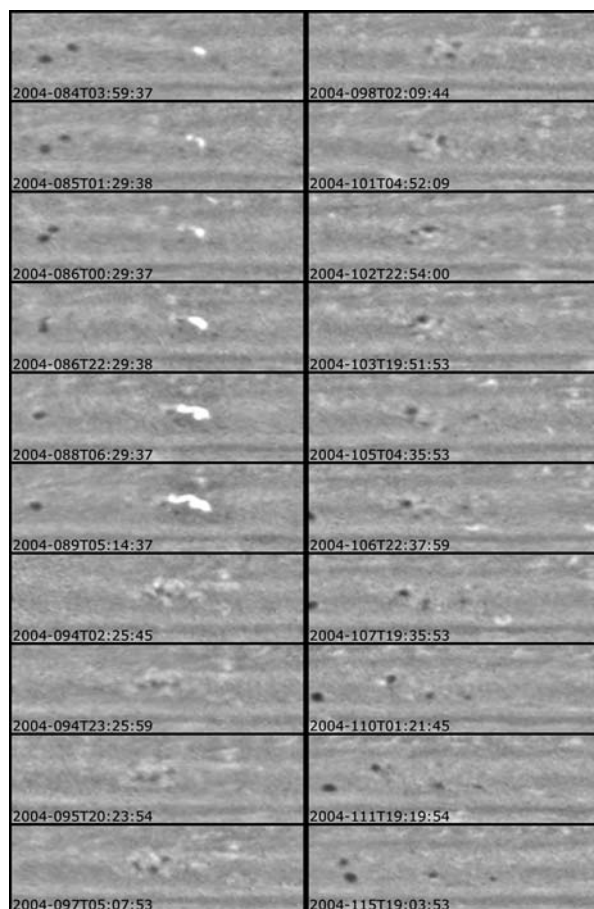
would suggest that the radio bursts are originating in the atmosphere and are probably caused by lightning discharges associated with the storm.
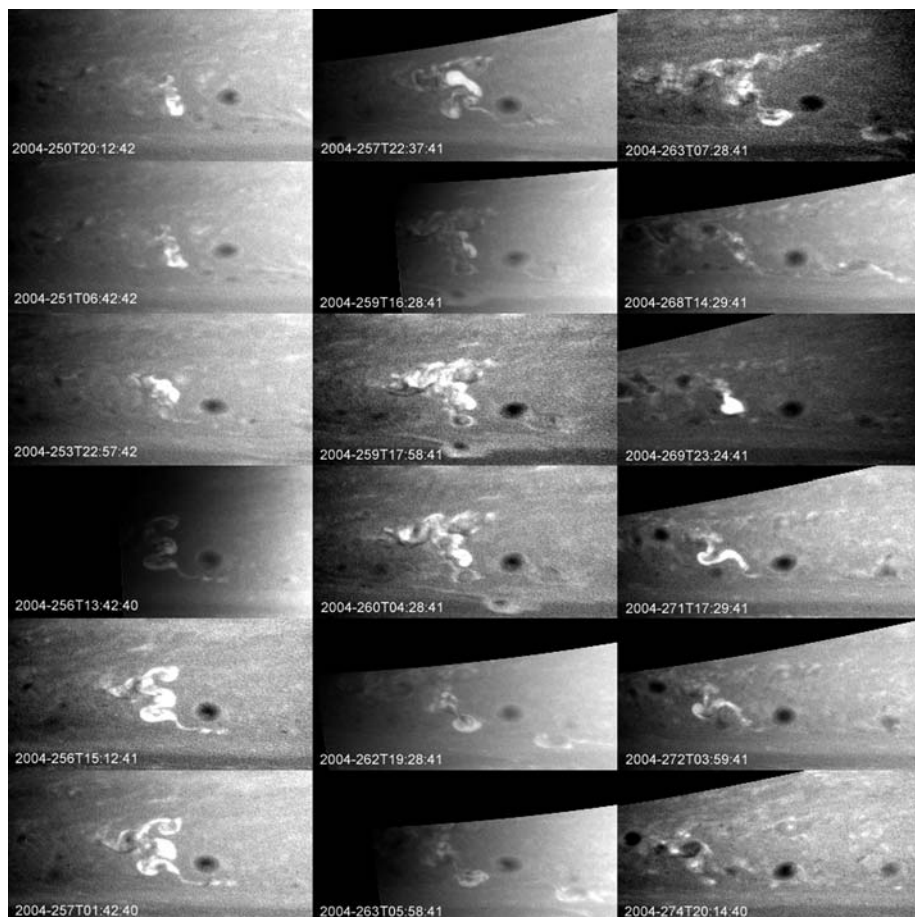
The results of this analysis are shown in Fig. 6. The SED "on" and "off" periods each last for ~5 hours, or ~0.5 planetary rotations. The bursts begin ~0.4 planetary rotations before the storm's CM crossing and end ~0.1 rotations after it (Fig. 6, insets). The phase of the SED episodes relative to the CM crossings remains constant and is the same for both outbursts, indicating that they are related. The maxima in the amplitude of the SED episodes (Fig. 6) at days 256 and 270 are correlated with an unusual brightening of the storm (Fig. 5), although the dynamic range of SED variation is greater than that of the storm brightness.

The peak SED intensity occurs ~0.2 planetary rotations (~72°) before the CM crossing, which suggests that the lightning source is ~72° to the east of the visible cloud, which trails off to the west because of wind shear. For this explanation to work, the lightning source would have to be deeper than the visible clouds and the wind would have to be more westward at higher altitude. Then the SEDs would lead the visible storm, as observed. Voyager 2 saw similar evidence of vertical shear in the zonal wind at almost the same latitude, but there the inference was that the winds were more eastward at higher altitude (1).

The two Voyagers detected low-frequency SED bursts—below 5 MHz—only when the spacecraft was above the night side of the planet (3, 25). If the ionospheric plasma density near the noon meridian was $\geq 3 \times 10^5$ cm^{-3}, escape of atmospheric radio bursts below 5 MHz would be prevented (3). If the nightside ionosphere had low-density regions or holes, the observed low-frequency emission could escape. This could explain the phase shift observed by Cassini, because the storm was in darkness before it crossed the CM and was in sunlight after CM crossing. The ionospheric cutoff would explain why SEDs appeared to turn off after the storm crossed the CM, but it does not explain why the SEDs began while the storm was still below the horizon (i.e., more than 0.25 rotations before CM crossing).

Fig. 5. Time sequence of the September storm at 35°S latitude. The sequence begins on day 250 (6 September 2004) and ends on day 274. The storm reaches its peak intensity in visible light on days 255 to 260. After fading for a few days, it returns as a high-contrast bright spot on day 269. Between day 272 and day 274, a dark filament appears and is observed curling up on its way to becoming a new dark spot.

References and Notes

1. A. P. Ingersoll, R. F. Beebe, B. J. Conrath, G. E. Hunt, in *Saturn*, T. Gehrels, M. S. Matthews, Eds. (Univ. of Arizona Press, Tucson, AZ, 1984), pp. 195–238.
2. A. Sánchez-Lavega, J. F. Rojas, P. V. Sada, *Icarus* **147**, 405 (2000).
3. M. L. Kaiser *et al.*, in *Saturn*, T. Gehrels, M. S. Matthews, Eds. (Univ. of Arizona Press, Tucson, AZ, 1984), pp. 378–415.
4. P. H. M. Galopeau, A. Lecacheux, *J. Geophys. Res.* **105**, 13089 (2000).
5. D. A. Gurnett *et al.*, *Science* **307**, 1255 (2004); published online 16 December 2004 (10.1126/science.1105356).
6. A. Sánchez-Lavega, S. Pérez-Hoyos, J. F. Rojas, R. Hueso, R. G. French, *Nature* **423**, 623 (2003).
7. A. Sánchez-Lavega, R. Hueso, S. Pérez-Hoyos, J. F. Rojas, R. G. French, *Icarus* **170**, 519 (2004).
8. The axial tilts of Jupiter and Saturn are 3.13° and 26.73°, respectively. Saturn's orbital period (and seasonal cycle) is 29.4 years.
9. B. Bézard, D. Gautier, B. Conrath, *Icarus* **60**, 274 (1984).
10. C. D. Barnet, J. A. Westphal, R. F. Beebe, L. F. Huber, *Icarus* **100**, 499 (1992).
11. A. Sánchez-Lavega *et al.*, *Nature* **353**, 397 (2000).
12. A. Sánchez-Lavega *et al.*, *Science* **271**, 631 (1996).
13. F. M. Flasar *et al.*, *Science* **307**, 1247 (2004); published online 23 December 2004 (10.1126/science.1105806).
14. A global map of Saturn, obtained by imaging Saturn's disk every 60° longitude as the planet rotated below the spacecraft, was acquired roughly every other rotation of Saturn. The spatial resolution of the narrow-angle camera ranged from 425 to 156 km per pixel. Images were navigated on the planetary limb, calibrated radiometrically, assembled into spatial mosaics, and mapped with a simple cylindrical projection. Illumination effects were removed by dividing the brightness value by the cosine of the solar incidence angle. Images from 29–30 May were part of a campaign to view Saturn at near-IR wavelengths.
15. C. C. Porco *et al.*, *Space Sci. Rev.* **115**, 363 (2004).
16. C. C. Porco *et al.*, *Science* **299**, 1541 (2003).
17. The solar phase angle was ~65°. The subsolar and subspacecraft planetocentric latitudes were –25° and –16°, respectively.
18. Winds were measured on images from 10–12 May, 29–30 May, and 6–7 September 2004. Spatial resolutions were ~157 km per pixel, ~104 km per pixel, and ~53 km per pixel, respectively, resulting in maximum wind speed precisions of 2.1 m s^{-1}, 1.4 m s^{-1}, and 0.7 m s^{-1}. Limited illumination and contrast within Saturn's cloud bands made identifying features more challenging than at Jupiter. Two authors (A.R.V., J.B.) tracked features with the use of different methods. One selected the initial and final tie points by eye. The other selected the feature by eye but used a digital correlation window to objectively determine the tie points.
19. R. A. West *et al.*, *Icarus* **51**, 51 (1982).
20. T. Temma *et al.*, *Icarus,* in press.
21. L. A. Sromovsky, H. E. Revercomb, R. J. Kraus, V. E. Suomi, *J. Geophys. Res.* **88**, 8650 (1983).
22. A. P. Ingersoll, P. J. Gierasch, D. Banfield, A. R. Vasavada, Galileo Imaging Team, *Nature* **403**, 630 (2000).
23. M. Desch and the RPWS team are acknowledged for the codiscovery of the correlation between the SEDs and Saturn convective storm activity and for allowing use of the data in figure 2 of Gurnett *et al.* (5).
24. J. A. Burns, M. R. Showalter, J. N. Cuzzi, R. H. Durisen, *Icarus* **54**, 280 (1983).
25. M. L. Kaiser, J. E. P. Connerney, M. D. Desch, *Nature* **303**, 50 (1983).
26. We acknowledge the many individuals across the imaging team who have assisted in the design of imaging sequences and camera commands and in other vital operational and image processing tasks, in particular N. Martin, J. Riley, E. Birath, B. Knowles, C. Clark, M. Belanger, and D. Wilson. Supported by NASA/JPL, the UK Particle Physics and Astronomy Research Council, the Deutsches Zentrum für Luft- und Raumfahrt (German Aerospace Center), and Université Paris VII Denis Diderot, Commissariat a l'Energie Atomique, Astrophysique Interactions Multiechelles, France.

Fig. 6. Timing of the storms' CM crossings relative to the timing of the SEDs. The abscissa is Universal Time at the space-craft; the labels refer to the start of each day. For the solid curves, the ordinate is the number of SED bursts per hour (5). The upper and lower panels represent different eruptions of the same storm; day 195 is 13 July 2004, and day 250 is 6 September 2004. On each image that contained the storm (a sighting), we measured the storm's longitude and computed when it would have crossed the CM on that saturnian day (Saturn rotation). Because we were looking at the dawn side of the planet, the CM crossings occurred before the storm sightings and are indicated by the positions of the asterisks along the abscissa. For images taken after day 250 (lower panel), we also computed the excess reflectivity [(storm/surroundings) − 1]. In this case the asterisk indicates not only the time of CM crossing (abscissa) but also the excess reflectivity of the storm (ordinate), in arbitrary units. Several asterisks at the same CM crossing represent several sightings of the storm on the same Saturn rotation. The different values of excess reflectivity (height of the asterisks) on the same Saturn rotation arise because the storm was observed at different positions on the half-illuminated disk. The coverage of the storms was intermittent, so gaps in the asterisks represent Saturn days when there were no observations. The coverage of SEDs was continuous, so gaps in the SED sequence represent Saturn days when there were no SEDs. The insets show the same data plotted versus Saturn time of day (Saturn's period is taken to be 10.6562 hours). Time 0.0 is when the storm is on the opposite side of the planet as viewed from Cassini; time 0.25 is the time at which the storm is rising above the horizon as seen by Cassini.
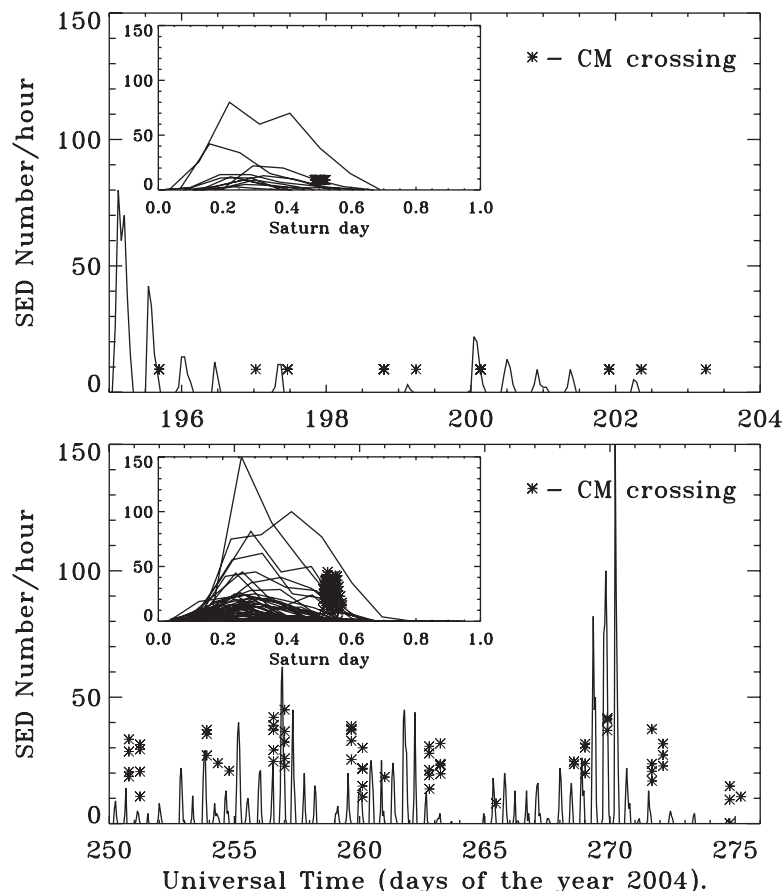
REPORT

Temperatures, Winds, and Composition in the Saturnian System

F. M. Flasar,[1]* R. K. Achterberg,[2] B. J. Conrath,[3] J. C. Pearl,[1] G. L. Bjoraker,[1] D. E. Jennings,[1] P. N. Romani,[1] A. A. Simon-Miller,[1] V. G. Kunde,[4] C. A. Nixon,[4] B. Bézard,[5] G. S. Orton,[6] L. J. Spilker,[6] J. R. Spencer,[7] P. G. J. Irwin,[8] N. A. Teanby,[8] T. C. Owen,[9] J. Brasunas,[1] M. E. Segura,[10] R. C. Carlson,[2] A. Mamoutkine,[2] P. J. Gierasch,[3] P. J. Schinder,[3] M. R. Showalter,[11] C. Ferrari,[12] A. Barucci,[5] R. Courtin,[5] A. Coustenis,[5] T. Fouchet,[5] D. Gautier,[5] E. Lellouch,[5] A. Marten,[5] R. Prangé,[5] D. F. Strobel,[13]† S. B. Calcutt,[8] P. L. Read,[8] F. W. Taylor,[8] N. Bowles,[8] R. E. Samuelson,[4] M. M. Abbas,[14] F. Raulin,[15] P. Ade,[16] S. Edgington,[6] S. Pilorz,[6] B. Wallis,[6] E. H. Wishnow[17]

Stratospheric temperatures on Saturn imply a strong decay of the equatorial winds with altitude. If the decrease in winds reported from recent Hubble Space Telescope images is not a temporal change, then the features tracked must have been at least 130 kilometers higher than in earlier studies. Saturn's south polar stratosphere is warmer than predicted from simple radiative models. The C/H ratio on Saturn is seven times solar, twice Jupiter's. Saturn's ring temperatures have radial variations down to the smallest scale resolved (100 kilometers). Diurnal surface temperature variations on Phoebe suggest a more porous regolith than on the jovian satellites.

Cassini observations of Saturn provide a detailed comparison with Jupiter, successfully studied by Galileo, which will sharpen our ideas about the formation of planetary systems. Each giant, fluid planet has its own system of orbiting moons. In addition, Saturn has a complex system of rings. All these objects are at temperatures in the range 55 to 200 K and radiate most of their energy at mid- and far-infrared wavelengths. In this part of

the spectrum, most molecules have distinctive fingerprints: manifolds of lines arising from rotational or vibrational-rotational transitions. Measuring the emitted radiation of these objects therefore probes their temperatures and composition.

The composite infrared spectrometer (CIRS) on Cassini consists of two Fourier-transform spectrometers, which together measure thermal emission from 10 to 1400 cm⁻¹ (wavelengths 1 mm to 7 μm) at an apodized spectral resolution selected between 0.5 and 15.5 cm⁻¹ (1, 2). The far-infrared interfer-ometer (10 to 600 cm⁻¹) has a 4-mrad field